Neuron 50, 23–33, April 6, 2006 ©2006 Elsevier Inc. DOI 10.1016/j.neuron.2006.02.026

# Ectopic Expression of a Microbial-Type Rhodopsin Restores Visual Responses in Mice with Photoreceptor Degeneration

**Anding Bi,[1] Jinjuan Cui,[1] Yu-Ping Ma,[1,4] Elena Olshevskaya,[2] Mingliang Pu,[3] Alexander M. Dizhoor,[1,2] and Zhuo-Hua Pan[1,*]**
[1] Department of Anatomy and Cell Biology
Wayne State University School of Medicine
Detroit, Michigan 48201
[2] Hafter Laboratories
Pennsylvania College of Optometry
Elkins Park, Pennsylvania 19027
[3] Department of Anatomy and Embryology
School of Basic Medical Sciences
Peking University
Beijing 100083
China

## Summary

**The death of photoreceptor cells caused by retinal degenerative diseases often results in a complete loss of retinal responses to light. We explore the feasibility of converting inner retinal neurons to photosensitive cells as a possible strategy for imparting light sensitivity to retinas lacking rods and cones. Using delivery by an adeno-associated viral vector, here, we show that long-term expression of a microbial-type rhodopsin, channelrhodopsin-2 (ChR2), can be achieved in rodent inner retinal neurons in vivo. Furthermore, we demonstrate that expression of ChR2 in surviving inner retinal neurons of a mouse with photoreceptor degeneration can restore the ability of the retina to encode light signals and transmit the light signals to the visual cortex. Thus, expression of microbial-type channelrhodopsins, such as ChR2, in surviving inner retinal neurons is a potential strategy for the restoration of vision after rod and cone degeneration.**

## Introduction

In the retina, photoreceptor cells convert light signals to electrical signals that are then relayed through second- and third-order retinal neurons to higher visual centers in the brain (Baylor, 1996; Wässle, 2004). The severe loss of photoreceptor cells caused by congenital retinal degenerative diseases, such as retinitis pigmentosa (RP) (Sung et al., 1991; Humphries et al., 1992; Weleber, 1994), often results in complete blindness. We explore the possibility of genetically converting the surviving inner retinal neurons into directly photosensitive cells—thus imparting light sensitivity to retinas that lack photoreceptors.

Critical to the feasibility of this strategy, it is required to have a suitable light-sensor. Previous studies reported the heterologous expression of *Drosophila* rhodopsin (Zemelman et al., 2002) and, more recently, melanopsin, the putative photopigment of the intrinsic photosensitive retinal ganglion cells (Melyan et al., 2005; Panda et al., 2005; Qiu et al., 2005). These photopigments, however, are coupled to membrane channels via a G protein signaling cascade and use *cis*-isoforms of retinaldehyde as their chromophore. As a result, expression of multiple genes would be required to render photosensitivity. In addition, their light response kinetics is rather slow. As part of an effort to improve the temporal resolution, recently a light-sensitive $K^+$ channel was engineered (Banghart et al., 2004). The latter technique, however, requires the introduction of an exogenous "molecular tether" and the use of UV light to unblock the channel. This engineered channel was proposed to be potentially useful for restoring light sensitivity in degenerate retinas, but its expression and function in retinal neurons remain unknown.

Our approach makes use of microbial-type rhodopsins similar to bacteriorhodopsin (Oesterhelt and Stoeckenius, 1973), whose conformation change is caused by reversible photoisomerization of their chromophore group, the all-*trans* isoform of retinaldehyde, and is directly coupled to ion movement through the membrane (Oesterhelt, 1998). Two microbial-type opsins, channelopsin-1 and -2 (Chop1 and Chop2), have recently been cloned from the green algae *Chlamydomonas reinhardtii* (Nagel et al., 2002; Sineshchekov et al., 2002; Nagel et al., 2003; Suzuki et al., 2003) and shown to form directly light-gated membrane channels when expressed in *Xenopus laevis* oocytes or HEK293 cells in the presence of all-*trans* retinal (Nagel et al., 2002, 2003). Chop2 is particularly attractive because its functional channel, channelrhodopsin-2 (ChR2, which refers to Chop2 with an attached chromophore), is permeable to physiological cations (Nagel et al., 2003). However, the long-term compatibility of expressing ChR2 in native neurons in vivo in general and the properties of ChR2-mediated light responses in retinal neurons in particular remain unknown.

Also essential to the feasibility of this strategy is the physiological state of surviving inner retinal neurons after photoreceptor degeneration. Histological studies, both in animal models of photoreceptor degeneration (Chang et al., 2002; Olshevskaya et al., 2004) and in postmortem patient eyes with almost complete photoreceptor loss because of RP (Santos et al., 1997; Milam et al., 1998), reported the preservation of a significant number of inner retinal neurons, but little is known about the physiological function of the surviving neurons. This is due, in part, to the lack of a photic stimulation tool once the photoreceptors have been lost. A detailed knowledge of the physiological capability of the degenerate retina is important because of the reports of remodeling of inner retinal neurons triggered by photoreceptor degeneration (Strettoi and Pignatelli 2000; Jones et al., 2003). Thus, ChR2 can serve not only for potential restoration of visual function but also as a powerful tool to probe the physiological status of the degenerate retina.

In this study, we investigated the feasibility of using ChR2 to restore light sensitivity to the retinas that have undergone rod and cone degeneration. We show that

*Correspondence: zhpan@med.wayne.edu
[4] Present address: Department of Pharmacology, Jiangsu University School of Medicine, Zhenjiang, Jiangsu 212013, China.

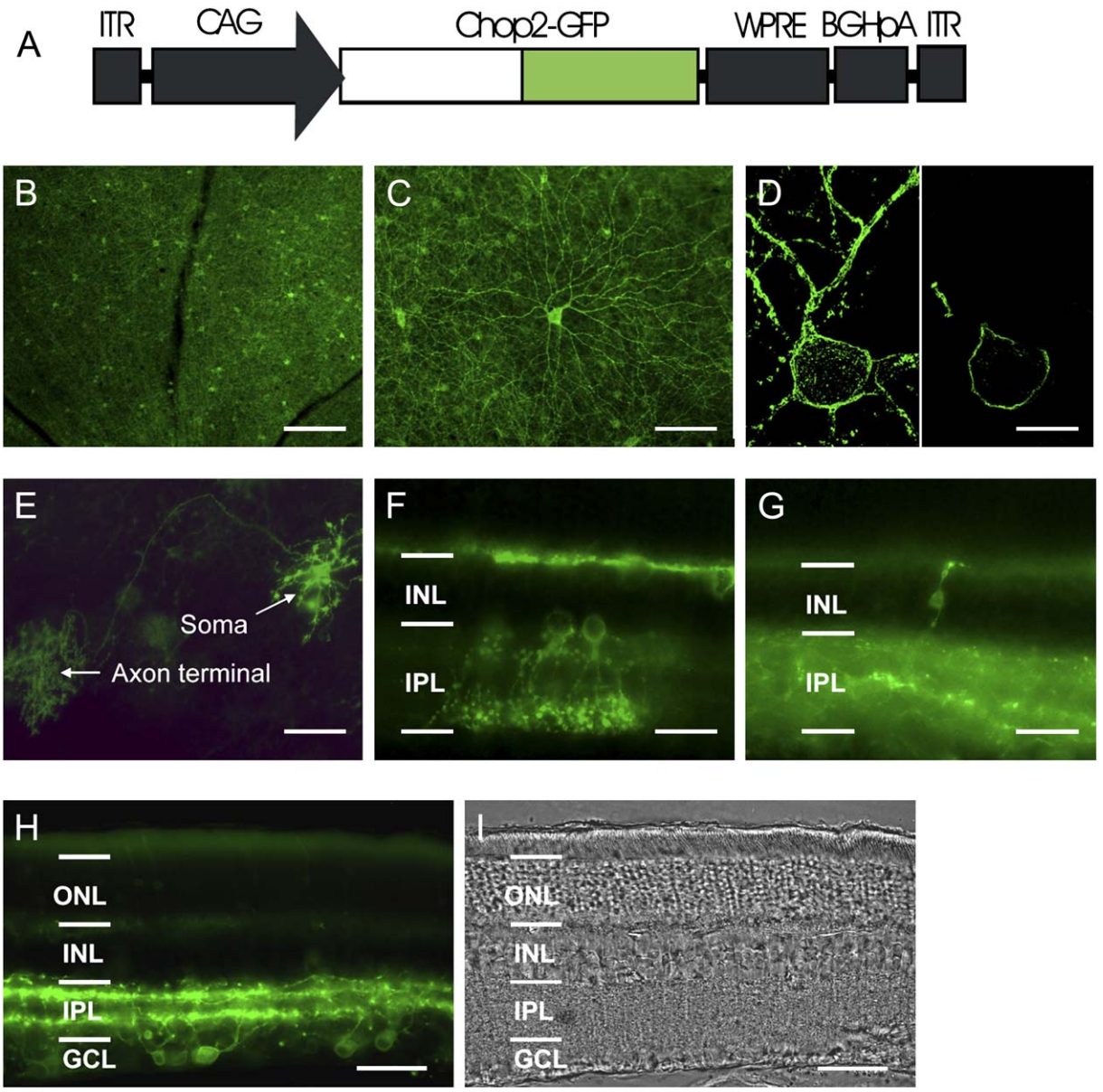


Figure 1. Expression of Chop2-GFP in Retinal Neurons In Vivo

(A) rAAV-CAG-Chop2-GFP-WPRE expression cassette. CAG: a hybrid CMV enhancer/chicken β-actin promoter. WPRE: woodchuck posttranscriptional regulatory element. BGHpA: a bovine growth hormone polyadenylation sequence.

(B and C) Chop2-GFP fluorescence viewed in low (B) and high (C) magnifications from eyes two months after the viral vector injection.

(D) Confocal images of a ganglion cell, which show a stacked image (left) and a single optical section image (right).

(E) Chop2-GFP fluorescence in a horizontal cell, which shows GFP in soma, axon, and distal axon terminal.

(F and G) Chop2-GFP fluorescence in amacrine cells (F) and a retinal bipolar cell (G).

(H and I) Fluorescence image (H) and phase contrast image (I) taken from a retina 12 months after the injection of Chop2-GFP viral vectors. Images in (B–E) were taken from flat whole-mounts of rat retinas. Images in (F–I) were taken from vertical slice sections of rat retinas. Scale bar: 200 μm in (B); 100 μm in (C); 15 μm in (D); 50 μm in (E), H), and (I); 25 μm in (F) and (G). ONL: outer nuclear layer; INL: inner nuclear layer; IPL: inner plexiform layer; GCL: ganglion cell layer.

long-term expression of ChR2 can be achieved in rodent inner retinal neurons in vivo. Our results also show that these inner retinal neurons can express a sufficient number of functional ChR2 channels to produce robust membrane depolarization or action potential firing without an exogenous supply of all-*trans* retinal. Furthermore, we demonstrate that the expression of ChR2 in a photoreceptor-deficient mouse model not only enables retinal ganglion cells to encode light signals but also restores visually evoked responses in the visual cortex.

## Results

### Expression of Chop2 in Retinal Neurons In Vivo

To directly visualize the expression and localization of Chop2 proteins, we replaced the C-terminal portion of the Chop2 channel with GFP, to make a Chop2-GFP

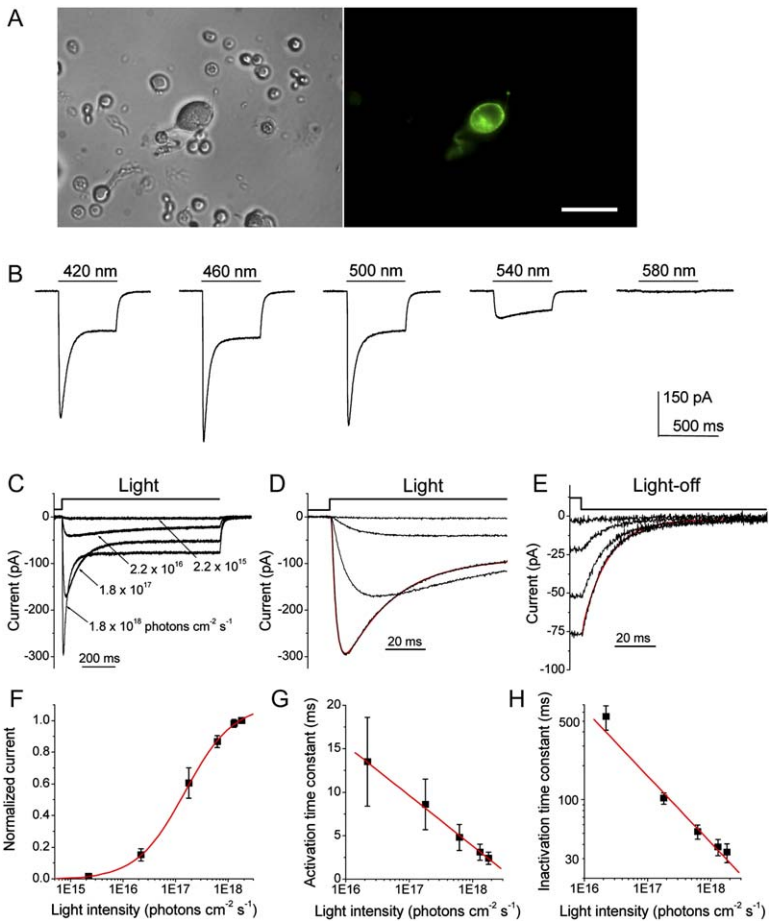


Figure 2. Properties of Light-Evoked Currents of the ChR2-Expressing Retinal Neurons

(A) Phase contrast image (left) and fluorescence image (right) of a GFP-positive retinal neuron dissociated from the viral vector injected eye. Scale bar: 25 μm.

(B) A recording of Chop2-GFP fluorescent retinal cell to light stimuli of wavelengths ranging from 420 to 580 nm. The light intensities were ranging from 1.0–1.6 × $10^{18}$ photons $cm^{-2}$ $s^{-1}$.

(C) A representative recording of the currents elicited by light stimuli at the wavelength of 460 nm with light intensities ranging from 2.2 × $10^{15}$ to 1.8 × $10^{18}$ photons $cm^{-2}$ $s^{-1}$.

(D) Current traces after the onset of the light stimulation from (C) shown in the expanded time scale. The red trace shows the fitting of one current trace by an exponential function: $I_{(t)} = a_0 + a_1 \times (1 - \exp[-t/\tau_1]) + a_2 \times (\exp[-t/\tau_2])$, in which $\tau_1$ and $\tau_2$ represent the activation and inactivation time constant, respectively.

(E) Current traces after the termination of the light stimulation from (C) shown in the expanded time scale. The red trace shows the fitting of one current trace by a single exponential function: $I_{(t)} = a_0 + a_1 \times (\exp[-t/\tau])$, in which $\tau$ represent the deactivation time constant.

(F) Light-intensity response curve. The data points were fitted with a single logistic function curve.

(G and H) The relationships of light-intensity and activation time constant (G) and light-intensity and inactivation time constant (H) obtained from the fitting shown in (D). All recordings were made at the holding potential of −70 mV. The data points in (F)–(H) are shown as mean ± SD (n = 7).

chimera. We chose the adeno-associated virus (AAV) vectors to target the expression of Chop2-GFP fusion protein into retinal neurons because the capability of AAV vectors to deliver transgenes into nondividing cells, including inner retinal neurons (Harvey et al., 2002; Martin et al., 2003), and to integrate the transgenes into the host genome (Flotte, 2004). A viral expression cassette, rAAV2-CAG-Chop2-GFP-WPRE, was made by subcloning the Chop2-GFP chimera into an AAV serotype-2 expression cassette containing a hybrid CMV enhancer/chicken β-actin (CAG) promoter (Figure 1A). To establish the expression and function of Chop2 channels in retinal neurons in general, we first examined the expression of Chop2 in nondystrophic retinas. The viral vector was injected into the intravitreal space in the eyes of postnatal day 1 rats and mice. Three to four weeks after the injection, bright GFP fluorescence was observed in retinal neurons of all injected eyes (Figures 1B–1H), confirming that Chop2-GFP was expressed. The expression was usually confluent throughout the retina (Figure 1B). The Chop2-GFP-fluorescence was predominantly observed in retinal ganglion cells (Figures 1C and 1D; also see Figure 1H). The fluorescence signal was observed throughout the inner plexiform layer (IPL) (Figure 1H), suggesting that the viral vector targeted the expression of Chop2-GFP both in ON and OFF ganglion cells. The expressing of Chop2-GFP was also frequently observed in horizontal cells (Figure 1E), amacrine cells (Figure 1F), and, occasionally, in bipolar cells (Figure 1G). The GFP signal was predominantly localized to the plasma membrane (Figure 1D), consistent with the GFP tag being anchored to the membrane by a seven-transmembrane portion of the Chop2 channel. Once expressed in a cell, the GFP signal was extended over the entire cell including distal processes and axon terminals (see Figures 1C and 1E). To date, bright GFP fluorescence has been found to be stable for 12 months after the injection (Figure 1H), whereas no gross changes in retinal morphology were noticed (Figure 1I). These results indicate that long-term stable expression of Chop2-GFP can be achieved in inner retinal neurons in vivo.

### Properties of Light-Evoked Currents of ChR2-Expressing Inner Retinal Neurons

We examined the functional properties of the Chop2 channels in inner retinal neurons by using whole-cell patch-clamp recordings. The recordings were performed in acutely dissociated cells so that photoreceptor-mediated light responses were confidently excluded. Chop2-GFP-positive cells were identified by their GFP fluorescence (Figure 2A). The precursor for the Chop2 chromophore group, all-*trans* retinal, was not added because it might be ubiquitously present in cells (Kim et al., 1992; Thompson and Gal, 2003). Light-evoked

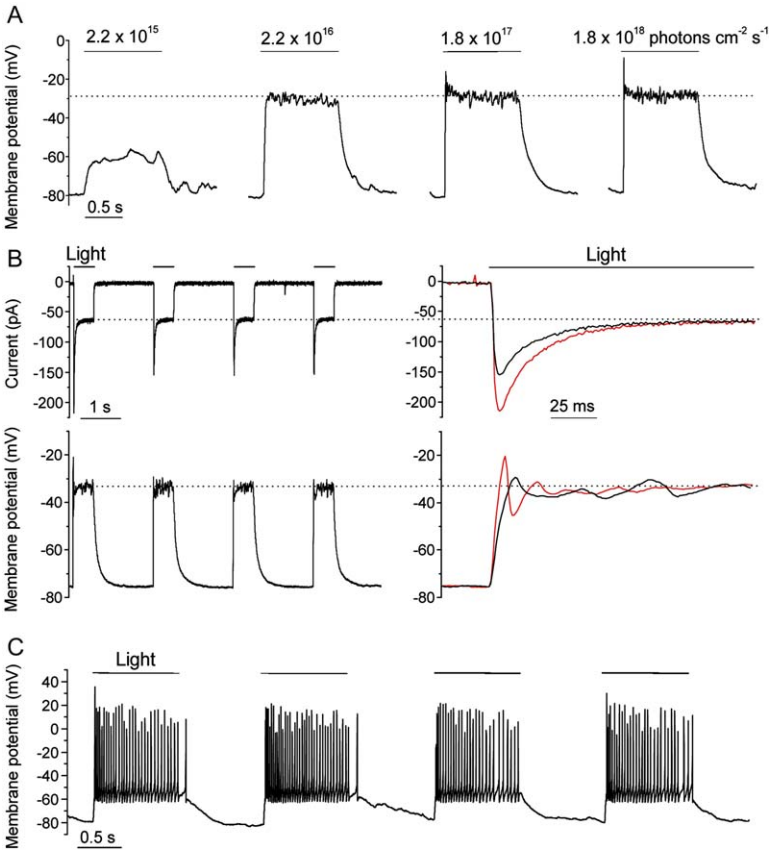


Figure 3. Properties of Light-Evoked Voltage Responses of ChR2-Expressing Retinal Neurons

(A) A representative recordings from GFP-positive nonspiking neurons. The voltage responses were elicited by four incremental light stimuli at the wavelength of 460 nm with intensities ranging from $2.2 \times 10^{15}$ to $1.8 \times 10^{18}$ photons $cm^{-2}\,s^{-1}$ in current clamp. The dotted line indicates the saturated potential level.

(B) A representative recording from GFP-positive nonspiking neurons to repeat light stimulations. The light-evoked currents (top traces) and voltage responses (bottom traces) from a same cells were shown. Left panel shows the superimposition of the first (red) and second (black) traces in an expanded time scale. The dotted line indicates the sustained component of the currents (top) and plateau membrane potential (bottom).

(C) A representative recording of GFP-positive spiking neurons to repeated light stimulations. The responses in (B) and (C) were evoked by light at the wavelength of 460 nm with the intensity of $1.8 \times 10^{18}$ photons $cm^{-2}\,s^{-1}$.

responses were observed in all recorded GFP fluorescent cells (n = 34), indicating that functional ChR2 (Chop2 with the chromophore attached) can be formed in retinal neurons with the retinal chromophore groups already present in the cells. Consistently, the expression of functional ChR2 channels has also been recently reported in cultured hippocampal neurons without the supply of exogenous retinal chromophore groups (Boyden et al., 2005; but see Li et al., 2005)

We first examined the properties of the ChR2-mediated light responses in voltage clamp. Light-evoked currents were observed in Chop2-GFP-expressing inner retinal neurons by light stimuli up to the wavelength of 580 nm with the most sensitive wavelength around 460 nm (Figure 2B), consistent with the reported peak spectrum sensitivity of ChR2 (Nagel et al., 2003). The amplitude and the kinetics of the currents were dependent on the light intensity (Figure 2C). Figures 2D and 2E show in the expanded time scale the current traces right after the onset and the termination of the light stimulation, respectively. Detectable currents were observed in most recorded cells at a light intensity of $2.2 \times 10^{15}$ photons $cm^{-2}\,s^{-1}$. In some cells, currents were observed at a light intensity of $2 \times 10^{14}$ photons $cm^{-2}\,s^{-1}$ (data not shown). At higher light intensities, the currents displayed both transient and sustained components, similar to the properties of the nonfusion ChR2 (Nagel et al., 2003). The relationship between the light intensity and peak current is shown in Figure 2F (n = 7). The activation and inactivation kinetics of the currents were also dependent on the light intensity (Figure 2D). The initial phase of the current could be well fitted by an exponential function with a single activation and inactivation constant, as illustrated in Figure 2D (red trace). The activation and inactivation time constants versus light intensity are plotted in Figures 2G and 2H, respectively. On the other hand, the deactivation kinetics of the currents after the light off was not light-intensity dependent. The current decay trace could be well fitted by a single exponential function as shown in Figure 2E (red trace). The time constant was 17.1 ± 6.5 ms (mean ± SD, n = 7).

We next examined whether the ChR2-mediated currents were sufficient to drive membrane depolarization. Figure 3A shows the representative responses from a nonspiking neuron in response to four incremental light intensities at the wavelength of 460 nm. Detectable responses were observed in most recorded cells at a light intensity of $2.2 \times 10^{15}$ photons $cm^{-2}\,s^{-1}$. At higher light intensities, the membrane depolarization approached a saturated level. We further examined the ChR2-mediated light responses to repeated light stimulations. The transient component of the currents diminished to repeated stimulations whereas the sustained component of the currents was stable (top traces in Figure 3B). This can be clearly seen in the expanded time scale in the right panel of Figure 3B by comparing the superimposed first (red trace) and the second (black trace) light-evoked currents. For the same cell, in current clamp, the stimulations evoked robust membrane depolarizations (bottom traces in Figure 3B). The membrane depolarizations reached an almost identical level, except for the initial portion of the response. This is also shown in the expanded time scale (right panel), which superimposes the first (red trace) and the second (black

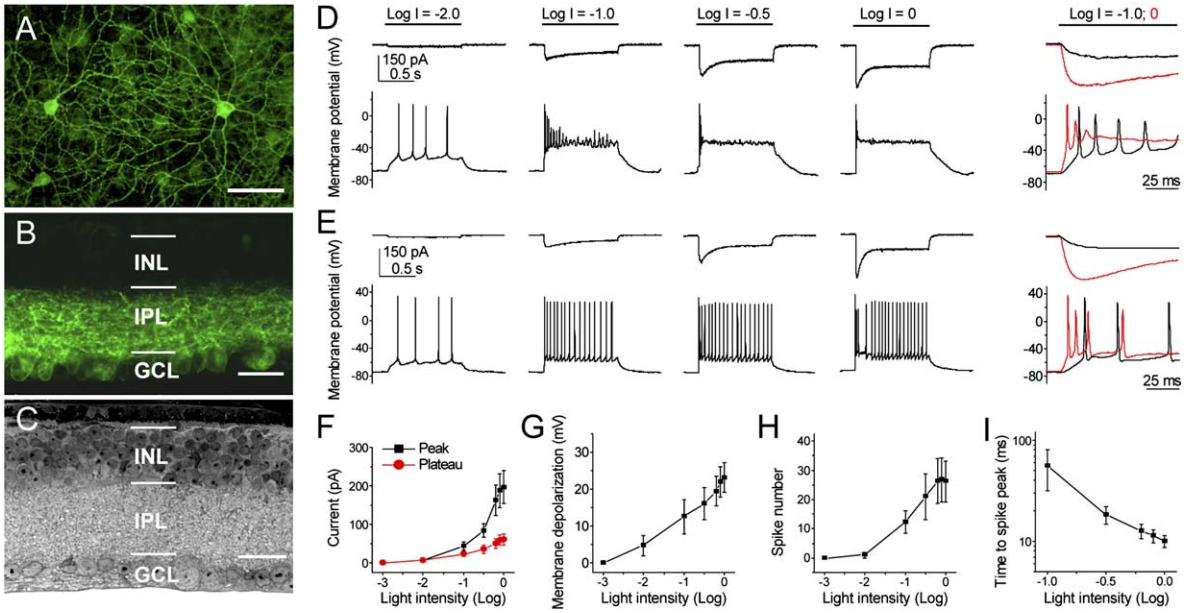


Figure 4. Expression and Light-Response Properties of ChR2 in Retinal Neurons of *rd1/rd1* Mice

(A) Chop2-GFP fluorescence viewed in flat retinal whole-mount of a 15 month old mouse with the Chop2-GFP viral vector injection at 3 months of age.

(B) Chop2-GFP fluorescence viewed in vertical section from the retina of a 6 month old mouse with the injection of Chop2-GFP viral vectors at 3 months of age.

(C) Light microscope image of a semithin vertical retinal section from a 5 month old mouse (Chop2-GFP viral vectors injected at postnatal day 1). Scale bar: 50 μm in (A) and 30 μm in (B) and (C).

(D–E) Representative recordings of transient spiking (D) and sustained spiking (E) GFP-positive neurons. The responses were elicited by light of four incremental intensities at the wavelength of 460 nm. The light intensity without neutral density (Log I = 0) was $3.6 \times 10^{17}$ photons $cm^{-2}$ $s^{-1}$. The currents were recorded at the holding potential of −70 mV. The superimposed second (black) and fourth (red) current and voltage traces are shown in the right panel in the expanded time scale.

(F–I) The relationships of the amplitude of current (F), membrane depolarization (G), the number of spikes (H), and the time to the first spike peak (I) to light intensity. Recordings were made from *rd1/rd1* mice at ≥4 months of age. The data points are shown as mean ± SE (n = 6 in [F]–[H] and n = 4 in [I]).

trace) light-evoked responses. Figure 3C shows a representative recording of spiking neurons to repeated light stimulations. Again, the stimulations elicited almost identical membrane depolarizations accompanied by multiple spikes. Taken together, these results demonstrate that the ChR2-mediated currents in second- and third-order retinal neurons are sufficient to drive membrane depolarization and/or spike firing.

### Expression of Chop2 in Photoreceptor-Deficient *rd1/rd1* Mice

Having established the expression and function of ChR2 in wild-type retinas, we went on to address whether the expression of ChR2 could restore light responses in retinas after photoreceptor degeneration. To this end, the experiments were carried out in homozygous *rd1* (*rd1/rd1*) mice (Bowes et al., 1990), a photoreceptor degeneration model with a null mutation in a cyclic GMP phosphodiesterase, PDE6, similar to some forms of retinitis pigmentosa in humans (McLaughlin et al., 1993). The Chop2-GFP viral vector was subvitreally injected into the eyes of newborn (P1) or adult mice at 2–12 months of age. Similar to the results observed in wild-type animals, bright GFP signal was observed in Chop2-GFP-injected retinas, predominately in retinal ganglion cells (Figures 4A and 4B). At the time of the recording experiments (≥4 months of age unless otherwise indicated), photoreceptor cells were absent (Figure 4C). The expression of Chop2-GFP was observed in the *rd1/rd1* mice up to 16 months of age (3–6 months after the viral injection) as the case shown in Figure 4A from a 15 month old *rd1/rd1* mouse. These results indicate that inner retinal neurons in this photoreceptor-deficient model not only survive long after the complete death of photoreceptors but also retain the capability of stable expression of Chop2-GFP.

### Light-Evoked Responses of ChR2-Expressing Surviving Inner Retinal Neurons of *rd1/rd1* Mice

We next examined the light response properties of the ChR2-expressing retinal neurons in *rd1/rd1* mice by whole-cell patch-clamp recording in retinal slices. The recordings were made from the GFP-positive cells located in the ganglion cell layer. Light-evoked currents were observed in GFP-positive cells. The magnitude of the current was again dependent on the light intensity (top traces in Figures 4D and 4E; also see light intensity and current relationships shown in Figure 4F). Two groups of ChR2-expressing retinal neurons were observed based on their response properties: a group of transient spiking neurons (Figure 4D) and a group of sustained spiking neurons (Figure 4E). The membrane depolarization and/or spike rates were also dependent on the light intensity (bottom traces in Figures 4D and

4E). Furthermore, light at higher intensities markedly accelerated the kinetics of the voltage responses as illustrated in the right panels of Figures 4D and 4E by superimposing the second traces (black) and the fourth traces (red) in an expanded time scale. The relationships of light intensity to the membrane depolarization, the spike firing rate, and the time to the first spike peak are shown in Figures 4G, 4H, and 4I, respectively. These results demonstrate that the surviving retinal third-order neurons with the expression of ChR2 are capable of encoding light intensity with membrane depolarization and/or action potential firing and response kinetics.

### Multielectrode Array Recordings of ChR2-Mediated Retinal Activities

We further examined the spike coding capability of the photoreceptor-deficient retina of *rd1/rd1* mice after the expression of ChR2 by use of multielectrode array recordings from whole-mount retinas. As shown from a sample recording in Figure 5A, spike firings with fast kinetics in response to light on and off were observed in Chop2-GFP-expressing retinas (n = 11 retinas). The light-evoked spike firings were not affected by the application of CNQX (25–50 μM) plus APV (25–50 μM) (n = 3), suggesting that the responses are originated from the ChR2 of the recorded cells. No such light-evoked spike firings were observed in retinas that were either injected with viral vectors carrying GFP alone (n = 2 retinas) or left uninjected (n = 3). The latter confirmed the absence of photoreceptor-originated light responses. The light-evoked spike firings were not affected by suramine (100 μM) (n = 2), which has been reported to be able to block melanopsin receptor-mediated photocurrent (Melyan et al., 2005; Qiu et al., 2005). In addition, the response kinetics to both light on and off (see Figure 5B) were much faster than those generated by the intrinsically photosensitive retinal ganglion cells (Tu et al., 2005). These results suggest that a significant contribution to the observed light responses from the intrinsically photosensitive ganglion cells under our recording conditions is unlikely. The light-evoked responses were often found to be picked up by the majority of the electrodes (see Figure 5A), consistent with the observation that Chop2-GFP was extensively expressed in the retinas. The vast majority of the responses were sustained during light stimulation. Figure 5B illustrates the raw traces recorded by a single electrode in response to three incremental light stimuli. The raster plots of the spike activity sorted from a single neuron of the recording were shown in Figure 5C. The firing frequency was remarkably stable during the course of the recording. The averaged spike rate histograms are shown in Figure 5D. Again, the spike frequency was increased to the higher light intensity. The light responses could be recorded for up to 5 hr. These results demonstrate further that the ChR2-expressing retinal ganglion cells can reliably encode light intensity with spike firing rate.

### Visual-Evoked Potentials

Finally, we asked whether the ChR2-mediated light responses in the retinas of *rd1/rd1* mice could be transmitted to the visual cortex. The expression of transgenes, such as GFP, in retinal ganglion cells as achieved by

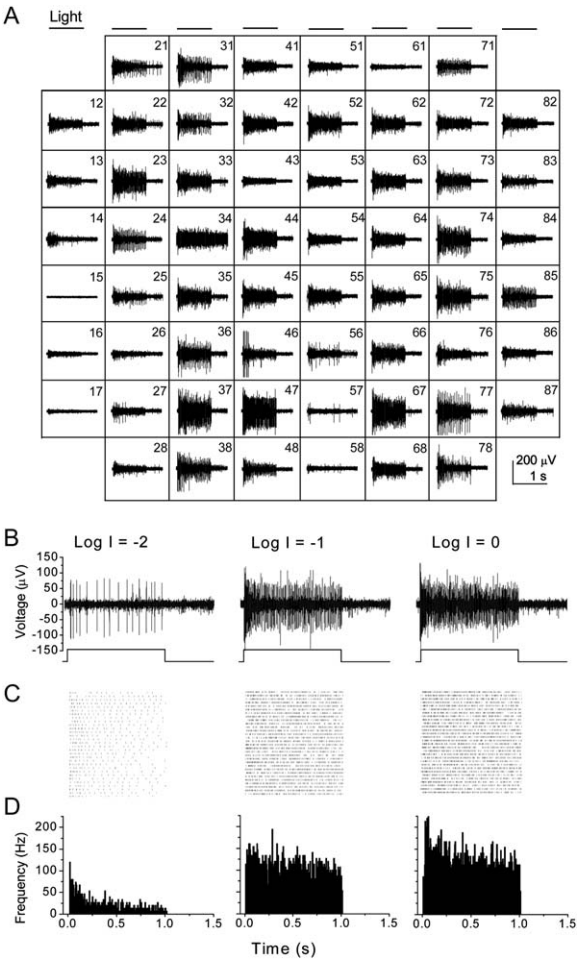


Figure 5. Multielectrode Array Recordings of the ChR2-Expressing Retinas of *rd1/rd1* Mice

(A) A sample recording of light-evoked spike activities from the retinas of *rd1/rd1* mice (ages ≥4 months). The recording was made in the present of CNQX (25 μM) and AP5 (25 μM). Prominent light-evoked spike activity was observed in 49 out of 58 electrodes (electrode 15 was for grounding and electrode 34 was defective).

(B) Sample light-evoked spikes recorded from a single electrode to three incremental light intensities.

(C) The raster plots of 30 consecutive light-elicited spikes originated from a single neuron.

(D) The averaged spike rate histograms. The light intensity without neutral density filters (Log I = 0) was $8.5 \times 10^{17}$ photons $cm^{-2}$ $s^{-1}$. The responses shown in (A) were elicited by a single light pulse without neutral density filters.

AAV infection was reported to be able to extend to their terminations in higher visual centers in the brain (Harvey et al., 2002). We, therefore, first examined the anatomical projections of the axon terminals of Chop2-GFP-expressing retinal ganglion cells. Consistently, Chop2-GFP labeled axon terminals of retinal ganglion cells were observed in several regions of the brain, including ventral lateral geniculate nucleus and dorsal lateral geniculate nucleus (Figure 6A), as well as superior colliculus (Figure 6B). These results suggest that the central projections of retinal ganglion cells in the degenerate retinas are maintained.

We then examined visual evoked potentials (VEPs) from visual cortex. First, as illustrated in Figure 6C,

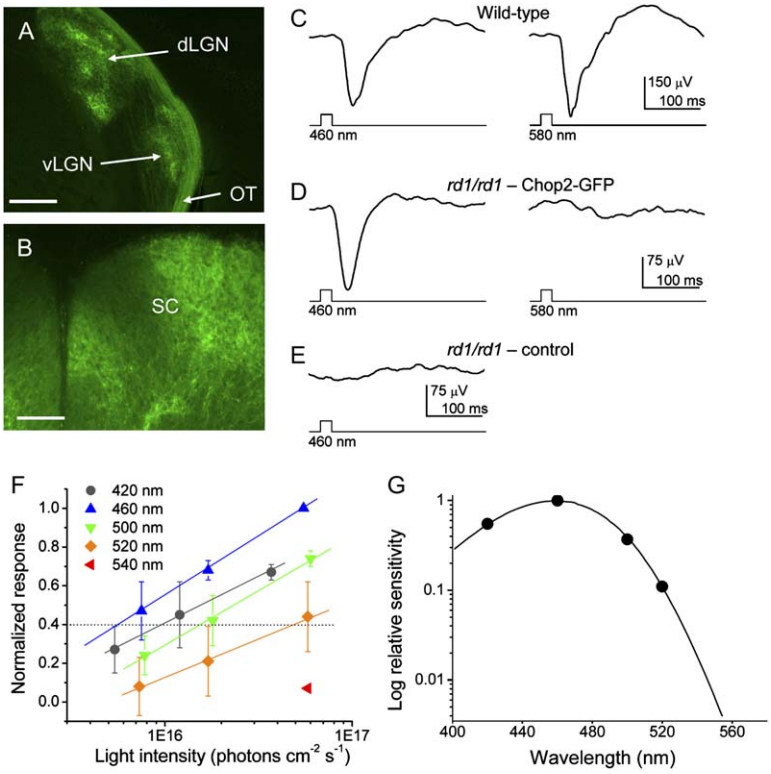


Figure 6. Central Projections of Chop2-GFP-Expressing Retinal Ganglion Cells and Visual-Evoked Potentials in *rd1/rd1* Mice

(A) GFP labeled terminal arbors of retinal ganglion cells in ventral lateral geniculate nucleus and dorsal lateral geniculate nucleus.

(B) GFP-labeled terminal arbors of retinal ganglion cells in superior colliculus. OT: optical track; vLGN: ventral lateral geniculate nucleus; dLGN: dorsal lateral geniculate nucleus; SC: superior colliculus. Scale bar: 200 μm in (A), 100 μm in (B).

(C) VEPs recorded from a wild-type mouse. The responses were observed both to the wavelengths of 460 and 580 nm.

(D) VEPs recorded from an *rd1/rd1* mouse injected with Chop2-GFP viral vectors. The responses were elicited only by light at the wavelength of 460 nm but not at the wavelength of 580 nm.

(E) No detectable VEPs were observed from *rd1/rd1* mice injected with viral vectors carrying GFP alone. The light intensities measured at the corneal surface at the wavelengths of 460 and 580 nm were $5.5 \times 10^{16}$ and $5.2 \times 10^{16}$ photons $cm^{-2}$ $s^{-1}$, respectively.

(F) Plot of the amplitude of VEPs from *rd1/rd1* mice injected with Chop2-GFP viral vectors to various light intensities at the wavelengths of 420, 460, 500, 520, and 540 nm. For each eye, the responses are normalized to the peak response obtained at 460 nm. The data are shown as mean ± SD (n = 3 eyes). Spectral sensitivity at each wavelength was defined as the inverse of the interpolated light intensity to produce 40% of the normalized peak response, as indicated by the dot line.

(G) The sensitivity data points are fitted by a vitamin-$A_1$-based visual pigment template with a peak wavelength of 461 nm.

VEPs were observed in all tested wild-type mice (4–6 months of age) in response to light stimuli at the wavelengths of both 460 and 580 nm (n = 6 eyes). When tested in Chop2-GFP-injected eyes of *rd1/rd1* mice (6–11 months of age), VEPs were observed in the majority of the eyes (nine out of 13) in response to light stimulus at the wavelength of 460 nm but not to light stimulus at the wavelength of 580 nm (Figure 6D), consistent with the light sensitivity of ChR2 channels (see Figure 2B). The average amplitude of the VEPs in the Chop2-GFP-injected eyes in response to the light stimulus at the wavelength of 460 nm was 110 ± 34 μV (mean ± SE; n = 10), which is smaller than that observed in wild-type mice (274 ± 113 μV; n = 6), although these two values are not significantly different (one-way ANOVA test, $p < 0.1$). The lower amplitudes of the VEPs in the Chop2-transfected mice compared to the wild-type mice are not surprising because the expression of ChR2 was probably only achieved in a small portion of the retinal ganglion cells. The average latency to the peak of the VEPs in the Chop2-GFP-injected eyes was 45 ± 1.7 ms (n = 10), which is shorter than that observed in wild-type mice (62 ± 2.8 ms; n = 6). These two values are significantly different ($p < 0.01$). The latter would be predicted because the light response mediated by ChR2 in retinal ganglion cells originates two synapses downstream of the photoreceptors. As a control, no detectable VEPs were observed to light stimulus at the wavelength of 460 nm in the eyes of the age-matched *rd1/rd1* mice that were injected with viral vectors carrying GFP alone (n = 5) (Figure 6E). In addition, no detectable VEPs were observed in uninjected *rd1/rd1* mice (n = 3; 5 months of age) to the wavelengths ranging from 420 to 620 nm (data not shown), confirming that *rd1/rd1* mice at ≥5 months of age are completely blind based on VEPs.

To further ensure that the VEPs in the blind *rd1/rd1* mice originate from ChR2 expressed in their retinas, we measured the action spectrum of the VEP by plotting their normalized amplitudes in response to varying light wavelengths and intensities to obtain the relative sensitivity of the response (Figure 6F) (n = 3). The data points were well fitted by a vitamin-$A_1$-based visual pigment template (Partridge and De Grip, 1991) with a peak wavelength at 461 nm (Figure 6G), a good match to the reported peak action spectrum of ChR2 at ~460 nm (Nagel et al., 2003). Taken together, these results demonstrate that expression of ChR2 in the photoreceptor-deficient retinas can restore visually evoked responses in the brain.

## Discussion

The results of this study demonstrate that the strategy of restoration of light responses in photoreceptor-deficient rodent retinas based on the expression of ChR2 is

mechanistically and technically feasible. Most importantly, our results show that ChR2 satisfies several major criteria for its use as a light sensor in retinal neurons. First, by delivery of an adeno-associated viral vector carrying fused Chop2-GFP, we show the ability of retinal neurons to tolerate the prolonged expression of Chop2. To date, the expression of Chop2-GFP proteins has been achieved in nondystrophic rat retinal neurons for 12 months and in photoreceptor deficient *rd1*/*rd1* mice for 6 months in vivo after the viral injection. Our results therefore suggest that the expression of ChR2 in retinal neurons is biocompatible under normal light cycle conditions. Second, our results show that a sufficient number of ChR2 can be formed in retinal neurons, with only endogenous chromophore groups as supplied by regular diet, to produce robust membrane depolarizations and/or action potential firings in the retina and VEPs in visual cortex. It is worth emphasizing here that, unlike animal visual pigments that rapidly lose their chromophore after its photoisomerization from 11-*cis* to all-*trans* retinal (Wald, 1968), for microbial-type rhodopsins, photoisomerization from all-*trans* to 11-*cis* retinal is reversible and both isomers remain attached to the protein (Oesterhelt, 1998). Once the ChR2 complex is formed, the light-sensitive channel can sustain multiple cycles of photoisomerization with the same chromophore moiety. Although the efficacy of the de novo ChR2 formation should depend on the availability of the chromophore group, the need for constant resupply of the chromophore to form new ChR2 does not appear to impose a limitation on overall ChR2 function. As observed in our multielectrode array recordings, ChR2 can respond repeatedly to light stimulation for several hours in vitro without loss of activity. Our results thus suggest that the turn-over rate for ChR2 is fairly slow, an additional advantage for using it as an artificially produced light sensor.

Furthermore, as reported originally in cell expression systems (Nagel et al., 2003), later in hippocampal neurons (Boyden et al., 2005; Ishizuka et al., 2006; Li et al., 2005), and now shown in retinal neurons, a number of properties of the ChR2 channel are highly advantageous for its use as a light sensor. First, the ChR2 channel is permeable to the cations that underlie neuronal membrane excitability. Thus, activation of ChR2 channels by light can directly produce membrane depolarizations to mimic the ON-responses of inner retinal neurons. Indeed, as shown in this study, the light-evoked responses mediated by ChR2 in nonspiking and spiking retinal neurons remarkably resemble the light responses of ON-bipolar cells and sustained ON-ganglion cells (Werblin and Dowling, 1969; Kaneko, 1970). Second, the activation kinetics of the current in response to light are extremely fast, whereas the sustained components of the currents do not show apparent inactivation to continuous or repeated light illuminations. Thus, the ChR2-expressing neurons can signal with rapid kinetics but without pigment inactivation. Consistently, the expression of ChR2 has been shown to allow optical control of neural excitability with high temporal resolution (Boyden et al., 2005; Ishizuka et al., 2006; Li et al., 2005). Furthermore, we show that the magnitude and activation kinetics of the light-evoked current are dependent on light irradiance over a 3-log-unit range. As demonstrated in our whole-cell and multielectrode array recordings, this would allow the encoding of various light intensities with graded membrane depolarizations and/or spike rates.

Also of importance for the feasibility of the strategy of restoring light sensitivity in retinas after photoreceptor degeneration, results of this study show that many inner retinal neurons survive in aged *rd1*/*rd1* mice (up to 16 months of age) and are capable of expressing ChR2 long after the death of all photoreceptors. This is consistent with histological studies showing that many inner retinal neurons survive, despite some remodeling, in this mouse model (Jimenez et al., 1996; Strettoi and Pignatelli 2000; Chang et al., 2002). Moreover, by using the ChR2 as a tool, we show in this study that the surviving inner retinal neurons retain their physiological capability to encode light signals with membrane depolarizations and/or action potential firings and to transmit visual signals to the visual cortex. Thus, the strategy based on the expression of ChR2 appears suitable at least for certain retinal degenerative diseases at certain degenerate stages. The remodeling of inner retinal neurons triggered by photoreceptor degeneration has raised some concerns for the retinal-based rescue strategy after the death of photoreceptors (Strettoi and Pignatelli 2000; Jones et al., 2003; Jones and Marc, 2005). However, retinal degenerative diseases are heterogeneous as to the time course of the degeneration, survival cell types, and, possibly, their functional state (Chang et al., 2002). Therefore, further studies are required to evaluate what types of retinal degenerative diseases and/or what disease stages are suitable for this potential treatment strategy. The use of ChR2 will be a powerful tool for undertaking such studies. It is worth mentioning here that the retinal remodeling is believed to be caused by deafferentation (Jones and Marc, 2005). Therefore, it would also be interesting to see if the restoration of the light sensitivity in inner retinal neurons could prevent or delay the remodeling processes.

Finally, viral-based gene delivery systems, such as AAV vectors (Flannery et al., 1997; Bennett et al., 1999; Ali et al., 2000; Acland et al., 2001), are promising tools for introducing Chop2 into retinal neurons as demonstrated in this study. For further studies, the combination of viral serotypes, cell-type specific promoters, and other regulatory factors could be used to develop optimized delivery vehicles for targeting of Chop2 to a specific functional subpopulation (or subpopulations) of surviving inner retinal neurons (Auricchio et al., 2001; Fitzsimons et al., 2002).

Results in this study show that that viral construct with AAV serotype-2 and CAG promoter can achieve robust expression of Chop2 in ganglion cells. However, because the expression of Chop2 with this construct appears to target both ON- and OFF-type ganglion cells, it remains to be determined how the conversion of both ON- and OFF-ganglion cells into ON-type affects the visual perception. Behavior studies in primates reported that pharmacological blockade of the ON channel in the retina did not severely impair such vision functions as the detection of light decrement and the perception of shape (Schiller et al., 1986). Therefore, if achievable, targeting of ChR2 to the ON channel, for example to ON-type ganglion cells, is more likely to result

in useful vision. A better approach would be to express ChR2 in the more distal retinal neurons, such as bipolar cells; this approach would utilize the remaining signal processing functions of the degenerate retina. Targeting ChR2 to rod bipolar cells is particularly attractive because the depolarization of rod bipolar cells can lead to the ON and OFF responses at the levels of cone bipolar cells and retinal ganglion cells (Wässle, 2004) and, thus, the ON and OFF channels that are inherent in the retina could be maintained.

It should be noted, however, that the threshold light intensity required for producing responses in ChR2-expressing retinas appeared to be near $10^{14}$–$10^{15}$ photons $cm^{-2}\,s^{-1}$. For comparison, the thresholds for normal rod and cone photoreceptors are about $10^{6}$ and $10^{10}$ photons $cm^{-2}\,s^{-1}$, respectively (Dacey et al., 2005). Therefore, the ChR2-expressing retinas would operate in substantially higher photonic range. The low light sensitivity of the ChR2-expressing retinas compared to the normal retinas could be due to a number of factors. First, there may be a low cross-sectional density of ChR2 molecules in the transfected retinal neurons compared with the visual pigments in rods and cones. Second, the ChR2-expressing inner retinal neurons lack the unique multilayer photoreceptor membrane organization, typical for the outer segments of rods and cones, which developed to achieve higher pigment density and thus increase the probability of catching photons (Steinberg, et al., 1980). Third, unlike visual pigments that propagate their signal through amplification cascade (Stryer, 1991), the directly light-gated ChR2 channels lack such amplification capabilities. Finally, in normal retinas, amplification of visual signals occurs as they converge from multiple photoreceptors to ganglion cells (Barlow et al., 1971), a process currently lacking in the ChR2-transfected retinas. Which of these factors contributes the most to the decreased light sensitivity of the ChR2-expressing retinas remains to be investigated. Interestingly, ChR2 was reported to mediate phototaxis to low-intensity light in green algae (Sineshchekov et al., 2002; but see Kateriya et al. [2004]). Therefore, it might be possible that the light sensitivity of ChR2 in retinal neurons was altered by modifications introduced in the Chop2 molecule for the heterologous expression. Such a difference may also reflect the profoundly different structural and functional organization of algae and mammalian cells. Nevertheless, for potential clinical usage, light intensifying devices can be used to expand the light operation range. Furthermore, it would be interesting for further study to use other microbial-type rhodopsins or to modify the light sensitivity of ChR2 as well as its other properties, such as ion selectivity and spectral sensitivity, to produce diversified light-sensitive channels to better fit the need for vision restoration.

At present, no treatment is available for restoring vision once the photoreceptor cells have been lost. Transplantation of normal photoreceptor cells or progenitor cells (Bok, 1993; Lund et al., 2001) or direct electrical stimulation of the surviving second- and third-order retinal neurons via retinal implants (Zrenner, 2002) are currently proposed as possible strategies for restoration of light responses in the retina after rod and cone degeneration. An important advantage of the strategy sought in this study is that it does not involve the introduction of tissues or devices into the retina and, therefore, may largely avoid the complications of immune reactions and biocompability. In addition, it could potentially achieve high spatial resolution for the restored "vision" because the approach targets the cellular level. Thus, the expression of microbial-type channelrhodopsins, such as ChR2, in surviving retinal neurons may be another potential strategy for the treatment of complete blindness caused by rod and cone degeneration.

## Experimental Procedures

### DNA and Viral Vector Constructions

The DNA fragment coding for the N-terminal fragment ($Met^{1}$-$Lys^{315}$) (Nagel et al., 2003) was cloned into pBluescript vector (Stratagene) containing the last exon of a mouse protamine 1 gene containing polyadenylation signal (mP1) and GFP cDNA inserted in frame at the 3′ end of the Chop2 coding fragment to produce a Chop2-GFP fusion protein. The function of Chop2-GFP chimera was verified in transfected HEK293 cells. The viral expression construct rAAV2-CAG-Chop2-GFP-WPRE was made by subcloning the Chop2-GFP fragment into an adeno-associated (serotype-2) viral expression cassette. The viral cassette contained a hybrid CMV enhancer/chicken β-actin promoter (CAG), a woodchuck posttranscriptional regulatory element (WPRE), and a bovine growth hormone (BGH) polyadenylation sequence. Viral vectors were packaged and affinity purified (GeneDetect).

### AAV Vector Injection

All of the animal experiments and procedures were approved by the Institutional Animal Care Committee at Wayne State University and were in accord with the NIH Guide for the Care and Use of Laboratory Animals. Newborn (P1) rat (Sprague-Dawley and Long-Evans) and mouse (C57/BL and C3H/HeJ or *rd1/rd1*) pups were anesthetized by chilling on ice. Adult mice (*rd1/rd1*) were anesthetized by intraperitoneal injection of the combination of katamine (100 mg/kg) and xylazine (10 mg/kg). Under a dissecting microscope, an incision was made by scissors through the eyelid to expose the sclera. A small perforation was made in the sclera region posterior to the lens with a needle and viral vector suspension of 0.8–1.5 μl at the concentration of $\sim 1 \times 10^{11}$ genomic particles/ml was injected into intravitreal space through the hole with a Hamilton syringe with a 32-gauge blunt-ended needle. For each animal, usually, only one eye was injected with viral vectors carrying Chop2-GFP and the other eye was uninjected or injected with viral vectors carrying GFP alone. After the injection, animals were kept on a 12/12 hr light/dark cycle. The light illumination of the room housing the animals measured at the wavelength of 500 nm was $6.0 \times 10^{14}$ photons $cm^{-2}\,s^{-1}$.

### Histology

Animals were sacrificed at various time points after the viral vector injection. The expression of Chop2-GFP fluorescence was examined in flat whole-mount retinas, vertical retinal, and coronal brain sections. The dissected retinas and brains were fixed with 4% paraformaldehyde in PBS for 0.5–2 hr at room temperature and 24 hr at 4ºC, respectively. The fixed retinas (embedded in 3% agarose) and brains were cut by using a vibratome. The retinal and brain sections or the retinal whole mounts were mounted on slides and covered with Vectashield medium (Vector Laboratories). GFP fluorescence was visualized under a fluorescence microscope equipped with exciter, dichroic, and emission filters of 465–495 nm, 505 nm, and 515–555 nm, respectively, and most images were obtained with a digital camera (Axiocam, Zeiss). Some images were obtained with a confocal microscope (TCS SP2, Leica). For light microscope of semithin vertical retinal section, eyes were enucleated, rinsed in PBS, and fixed in 1% osmium tetroxide, 2.5% glutaraldehyde, and 0.2 M Sorenson' s phosphate buffer (pH 7.4) at 4ºC for 3 hr. The eyes were then dehydrated in graded ethanols and embedded in plastic and cut into 1 μm thick sections and stained with a methylene blue/azure mixture.

### Patch-Clamp Recordings

Dissociated retinal cells and retinal slice were prepared as previously described (Pan, 2000; Cui et al., 2003). Recordings with patch electrodes in the whole-cell configuration were made by an EPC-9 amplifier and PULSE software (Heka Electronik, Lambrecht, Germany). Recordings were made in a Hanks' solution containing (in mM): NaCl, 138; $NaHCO_3$, 1; $Na_2HPO_4$, 0.3; KCl, 5; $KH_2PO_4$, 0.3; $CaCl_2$, 1.25; $MgSO_4$, 0.5; $MgCl_2$, 0.5; HEPES-NaOH, 5; glucose, 22.2; with phenol red, 0.001% v/v; adjusted to pH 7.2 with 0.3 N NaOH. The electrode solution contained (in mM): K-gluconate, 133; KCl, 7; $MgCl_2$, 4; EGTA, 0.1; HEPES, 10; Na-GTP, 0.5; and Na-ATP, 2; pH adjusted with KOH to 7.4. The resistance of the electrode was 13 to 15 MΩ. The recordings were performed at room temperature (~22ºC).

### Multielectrode Array Recordings

The multielectrode array recordings were based on the procedures reported by Tian and Copenhagen (2003). Briefly, the retina was dissected and placed photoreceptor side down on a piece of nitrocellulose filter paper (Millipore Corp., Bedford, MA). The mounted retina was placed in the MEA-60 multielectrode array recording chamber of 30 μm diameter electrodes spaced 200 μm apart (Multi Channel System MCS GmbH, Reutlingen, Germany), with the ganglion cell layer facing the recording electrodes. The retina was continuously perfused in oxygenated extracellular solution at 34ºC during all experiments. The extracellular solution contained (in mM): NaCl, 124; KCl, 2.5; $CaCl_2$, 2; $MgCl_2$, 2; $NaH_2PO_4$, 1.25; $NaHCO_3$, 26; and glucose, 22 (pH 7.35 with 95% $O_2$ and 5% $CO_2$). Recordings were usually started 60 min after the retina was positioned in the recording chamber. The interval between onsets of each light stimulus was 10–15 s. The signals were filtered between 200 Hz (low cut off) and 20 kHz (high cut off). The responses from individual neurons were analyzed by using Offline Sorter software (Plexon, Inc., Dallas, TX).

### Visual-Evoked Potential Recordings

Visual-evoked potential recordings were carried out in wild-type mice (C57BL/6 and 129/SV) at 4–6 months of age and in the *rd1/rd1* mice at 6–11 months of age and 2–6 months after the viral vector injection. After being anesthetized by intraperitoneal injection of the combination of katamine (100 mg/kg) and acepromazine (0.8 mg/kg), animals were mounted in a stereotaxic apparatus. Body temperature was either maintained at 34°C with a heating pat and a rectal probe or unregulated. Pupils were dilated by 1% atropine and 2.5% accu-phenylephrine. A small portion of the skull (~1.5 × 1.5 mm) centered about 2.5 mm from the midline and 1 mm rostral to the lambdoid suture was drilled and removed. Recordings were made from visual cortex (area V1) by a glass micropipette (resistance about 0.5 M after filled with 4 M NaCl) advanced 0.4 mm beneath the surface of the cortex at the contralateral side of the stimulated eye. The stimuli were 20 ms pluses at 0.5 Hz. Responses were amplified (1,000 to 10,000), band-pass filtered (0.3–100 Hz), digitized (1 kHz), and averaged between 30–250 trials.

### Light Stimulation

For dissociated cell and retinal slice recordings, light stimuli were generated by a 150 W xenon lamp-based scanning monochromator with bandwidth of 10 nm (TILL Photonics, Germany) and coupled to the microscope with an optical fiber. For multielectrode array recordings, light responses were evoked by the monochromator or a 175 W xenon lamp-based illuminator (Lambda LS, Sutter Instrument) with a band-pass filter of 400–580 nm and projected to the bottom of the recording chamber through a liquid light guider. For visual evoked potential, light stimuli were generated by the monochromator and projected to the eyes through the optical fiber. The light intensity was attenuated by neutral density filters. The light energy was measured by a thin-type sensor (TQ82017) and an optical power meter (Model: TQ8210) (Advantest, Tokyo, Japan).

### Acknowledgments

We thank Dr. R. Pourcho for critically reading the manuscript; Drs. S.A. Lipton, M.M. Slaughter, J. Hurley, N. Tian, R. Andrade, L.D. Hazlett for helpful comments on the manuscript; and R. Barrett for technical assistance. We also thank Dr. N. Tian for help in setting up the multielectrode array recording system. This work was supported by National Institutes of Health grants EY12180 and EY16087 to Z.-H.P., EY11522 and Pennsylvania Department of Health to A.M.D., and core grant EY04068 to Department of Anatomy and Cell Biology at Wayne State University.

Received: November 29, 2005
Revised: January 12, 2006
Accepted: February 23, 2006
Published: April 5, 2006

### References

Acland, G.M., Aguirre, G.D., Ray, J., Zhang, Q., Aleman, T.S., Cideciyan, A.V., Pearce-Kelling, S.E., Anand, V., Zeng, Y., Maguire, A.M., et al. (2001). Gene therapy restores vision in a canine model of childhood blindness. Nat. Genet. *28*, 92–95.

Ali, R.R., Sarra, G.M., Stephens, C., Alwis, M.D., Bainbridge, J.W., Munro, P.M., Fauser, S., Reichel, M.B., Kinnon, C., Hunt, D.M., et al. (2000). Restoration of photoreceptor ultrastructure and function in retinal degeneration slow mice by gene therapy. Nat. Genet. *25*, 306–310.

Auricchio, A., Kobinger, G., Anand, V., Hildinger, M., O' Connor, E., Maguire, A.M., Wilson, J.M., and Bennett, J. (2001). Exchange of surface proteins impacts on viral vector cellular specificity and transduction characteristics: the retina as a model. Hum. Mol. Genet. *10*, 3075–3081.

Banghart, M., Borges, K., Isacoff, E., Trauner, D., and Kramer, R.H. (2004). Light-activated ion channels for remote control of neuronal firing. Nat. Neurosci. *7*, 1381–1386.

Barlow, H.B., Levick, W.R., and Yoon, M. (1971). Responses to single quanta of light in retinal ganglion cells of the cat. Vision Res. *3*, 87–101.

Baylor, D. (1996). How photons start vision. Proc. Natl. Acad. Sci. USA *93*, 560–565.

Bennett, J., Maguire, A.M., Cideciyan, A.V., Schnell, M., Glover, E., Anand, V., Aleman, T.S., Chirmule, N., Gupta, A.R., Huang, Y., et al. (1999). Stable transgene expression in rod photoreceptors after recombinant adeno-associated virus-mediated gene transfer to monkey retina. Proc. Natl. Acad. Sci. USA *96*, 9920–9925.

Bok, D. (1993). Retinal transplantation and gene therapy. Present realities and future possibilities. Invest. Ophthalmol. Vis. Sci. *34*, 473–476.

Bowes, C., Li, T., Danciger, M., Baxter, L.C., Applebury, M.L., and Farber, D.B. (1990). Retinal degeneration in the rd mouse is caused by a defect in the beta subunit of rod cGMP-phosphodiesterase. Nature *347*, 677–680.

Boyden, E.S., Zhang, F., Bamberg, E., Nagel, G., and Deisseroth, K. (2005). Millisecond-timescale, genetically targeted optical control of neural activity. Nat. Neurosci. *8*, 1263–1268.

Chang, B., Hawes, N.L., Hurd, R.E., Davisson, M.T., Nusinowitz, S., and Heckenlively, J.R. (2002). Retinal degeneration mutants in the mouse. Vision Res. *42*, 517–525.

Cui, J., Ma, Y.P., Lipton, S.A., and Pan, Z.-H. (2003). Glycine receptors and glycinergic synaptic input at the axon terminals of mammalian retinal rod bipolar cells. J. Physiol. *553*, 895–909.

Dacey, D.M., Liao, H.W., Peterson, B.B., Robinson, F.R., Smith, V.C., Pokorny, J., Yau, K.W., and Gamlin, P.D. (2005). Melanopsin-expressing ganglion cells in primate retina signal colour and irradiance and project to the LGN. Nature *433*, 749–754.

Fitzsimons, H.L., Bland, R.J., and During, M.J. (2002). Promoters and regulatory elements that improve adeno-associated virus transgene expression in the brain. Methods *28*, 227–236.

Flannery, J.G., Zolotukhin, S., Vaquero, M.I., LaVail, M.M., Muzyczka, N., and Hauswirth, W.W. (1997). Efficient photoreceptor-targeted gene expression in vivo by recombinant adeno-associated virus. Proc. Natl. Acad. Sci. USA *94*, 6916–6921.

Flotte, T.R. (2004). Gene therapy progress and prospects: recombinant adeno-associated virus (rAAV) vectors. Gene Ther. *11*, 805–810.

Harvey, A.R., Kamphuis, W., Eggers, R., Symons, N.A., Blits, B., Niclou, S., Boer, G.J., and Verhaagen, J. (2002). Intravitreal injection of adeno-associated viral vectors results in the transduction of different types of retinal neurons in neonatal and adult rats: a comparison with lentiviral vectors. Mol. Cell. Neurosci. *21*, 141–157.

Humphries, P., Kenna, P., and Farrar, G.J. (1992). On the molecular genetics of retinitis pigmentosa. Science *256*, 804–808.

Ishizuka, T., Kakuda, M., Araki, R., and Yawo, H. (2006). Kinetic evaluation of photosensitivity in genetically engineered neurons expressing green algae light-gated channels. Neurosci. Res. *54*, 85–94.

Jimenez, A.J., Garcia-Fernandez, J.M., Gonzalez, B., and Foster, R.G. (1996). The spatio-temporal pattern of photoreceptor degeneration in the aged rd/rd mouse retina. Cell Tissue Res. *284*, 193–202.

Jones, B.W., and Marc, R.E. (2005). Retinal remodeling during retinal degeneration. Exp. Eye Res. *81*, 123–137.

Jones, B.W., Watt, C.B., Frederick, J.M., Baehr, W., Chen, C.K., Levine, E.M., Milam, A.H., Lavail, M.M., and Marc, R.E. (2003). Retinal remodeling triggered by photoreceptor degenerations. J. Comp. Neurol. *464*, 1–16.

Kaneko, A. (1970). Physiological and morphological identification of horizontal, bipolar, and amacrine cells in the goldfish retina. J. Physiol. *207*, 623–633.

Kateriya, S., Nagel, G., Bamberg, E., and Hegemann, P. (2004). "Vision" in single-celled algae. News Physiol. Sci. *19*, 133–137.

Kim, C.I., Leo, M.A., and Lieber, C.S. (1992). Retinol forms retinoic acid via retinal. Arch. Biochem. Biophys. *294*, 388–393.

Li, X., Gutierrez, D.V., Hanson, M.G., Han, J., Mark, M.D., Chiel, H., Hegemann, P., Landmesser, L.T., and Herlitze, S. (2005). Fast noninvasive activation and inhibition of neural and network activity by vertebrate rhodopsin and green algae channelrhodopsin. Proc. Natl. Acad. Sci. USA *102*, 17816–17821.

Lund, R.D., Kwan, A.S., Keegan, D.J., Sauve, Y., Coffey, P.J., and Lawrence, J.M. (2001). Cell transplantation as a treatment for retinal disease. Prog. Retin. Eye Res. *20*, 415–449.

Martin, K.R., Quigley, H.A., Zack, D.J., Levkovitch-Verbin, H., Kielczewski, J., Valenta, D., Baumrind, L., Pease, M.E., Klein, R.L., and Hauswirth, W.W. (2003). Gene therapy with brain-derived neurotrophic factor as a protection: retinal ganglion cells in a rat glaucoma model. Invest. Ophthalmol. Vis. Sci. *44*, 4357–4365.

McLaughlin, M.E., Sandberg, M.A., Berson, E.L., and Dryja, T.P. (1993). Recessive mutations in the gene encoding the beta-subunit of rod phosphodiesterase in patients with retinitis pigmentosa. Nat. Genet. *4*, 130–134.

Melyan, Z., Tarttelin, E.E., Bellingham, J., Lucas, R.J., and Hankins, M.W. (2005). Addition of human melanopsin renders mammalian cells photoresponsive. Nature *433*, 741–745.

Milam, A.H., Li, Z.Y., and Fariss, R.N. (1998). Histopathology of the human retina in retinitis pigmentosa. Prog. Retin. Eye Res. *17*, 175–205.

Nagel, G., Ollig, D., Fuhrmann, M., Kateriya, S., Musti, A.M., Bamberg, E., and Hegemann, P. (2002). Channelrhodopsin-1: a light-gated proton channel in green algae. Science *296*, 2395–2398.

Nagel, G., Szellas, T., Huhn, W., Kateriya, S., Adeishvili, N., Berthold, P., Ollig, D., Hegemann, P., and Bamberg, E. (2003). Channelrhodopsin-2, a directly light-gated cation-selective membrane channel. Proc. Natl. Acad. Sci. USA *100*, 13940–13945.

Oesterhelt, D. (1998). The structure and mechanism of the family of retinal proteins from halophilic archaea. Curr. Opin. Struct. Biol. *8*, 489–500.

Oesterhelt, D., and Stoeckenius, W. (1973). Functions of a new photoreceptor membrane. Proc. Natl. Acad. Sci. USA *70*, 2853–2857.

Olshevskaya, E.V., Calvert, P.D., Woodruff, M.L., Peshenko, I.V., Savchenko, A.B., Makino, C.L., Ho, Y.S., Fain, G.L., and Dizhoor, A.M. (2004). The Y99C mutation in guanylyl cyclase-activating protein 1 increases intracellular $Ca^{2+}$ and causes photoreceptor degeneration in transgenic mice. J. Neurosci. *24*, 6078–6085.

Pan, Z.-H. (2000). Differential expression of high- and two types of low-voltage-activated calcium currents in rod and cone bipolar cells of the rat retina. J. Neurophysiol. *83*, 513–527.

Panda, S., Nayak, S.K., Campo, B., Walker, J.R., Hogenesch, J.B., and Jegla, T. (2005). Illumination of the melanopsin signaling pathway. Science *307*, 600–604.

Partridge, J.C., and De Grip, W.J. (1991). A new template for rhodopsin (vitamin $A_1$ based) visual pigments. Vision Res. *31*, 619–630.

Qiu, X., Kumbalasiri, T., Carlson, S.M., Wong, K.Y., Krishna, V., Provencio, I., and Berson, D.M. (2005). Induction of photosensitivity by heterologous expression of melanopsin. Nature *433*, 745–749.

Santos, A., Humayun, M.S., de Juan, E., Jr., Greenburg, R.J., Marsh, M.J., Klock, I.B., and Milam, A.H. (1997). Preservation of the inner retina in retinitis pigmentosa. A morphometric analysis. Arch. Ophthalmol. *115*, 511–515.

Schiller, P.H., Sandell, J.H., and Maunsell, J.H. (1986). Functions of the ON and OFF channels of the visual system. Nature *322*, 824–825.

Sineshchekov, O.A., Jung, K.H., and Spudich, J.L. (2002). Two rhodopsins mediate phototaxis to low- and high-intensity light in *Chlamydomonas reinhardtii*. Proc. Natl. Acad. Sci. USA *99*, 8689–8694.

Steinberg, R.H., Fisher, S.K., and Anderson, D.H. (1980). Disc morphogenesis in vertebrate photoreceptors. J. Comp. Neurol. *190*, 501–518.

Strettoi, E., and Pignatelli, V. (2000). Modifications of retinal neurons in a mouse model of retinitis pigmentosa. Proc. Natl. Acad. Sci. USA *97*, 11020–11025.

Stryer, L. (1991). Visual excitation and recovery. J. Biol. Chem. *266*, 10711–10724.

Sung, C.H., Davenport, C.M., Hennessey, J.C., Maumenee, I.H., Jacobson, S.G., Heckenlively, J.R., Nowakowski, R., Fishman, G., Gouras, P., and Nathans, J. (1991). Rhodopsin mutations in autosomal dominant retinitis pigmentosa. Proc. Natl. Acad. Sci. USA *88*, 6481–6485.

Suzuki, T., Yamasaki, K., Fujita, S., Oda, K., Iseki, M., Yoshida, K., Watanabe, M., Daiyasu, H., Toh, H., Asamizu, E., et al. (2003). Archaeal-type rhodopsins in *Chlamydomonas*: model structure and intracellular localization. Biochem. Biophys. Res. Commun. *301*, 711–717.

Tian, N., and Copenhagen, D.R. (2003). Visual stimulation is required for refinement of ON and OFF pathways in postnatal retina. Neuron *39*, 85–96.

Thompson, D.A., and Gal, A. (2003). Vitamin A metabolism in the retinal pigment epithelium: genes, mutations, and diseases. Prog. Retin. Eye Res. *22*, 683–703.

Tu, D.C., Zhang, D., Demas, J., Slutsky, E.B., Provencio, I., Holy, T.E., and Van Gelder, R.N. (2005). Physiologic diversity and development of intrinsically photosensitive retinal ganglion cells. Neuron *48*, 987–999.

Wald, G. (1968). The molecular basis of visual excitation. Nature *219*, 800–807.

Wässle, H. (2004). Parallel processing in the mammalian retina. Nat. Rev. Neurosci. *5*, 747–757.

Weleber, R.G. (1994). Retinitis pigmentosa and allied disorders. In Retina, S.J. Ryan, ed. (St. Louis, MO: Mosby), pp. 335–466.

Werblin, F.S., and Dowling, J.E. (1969). Organization of the retina of the mudpuppy, Necturus maculosus. II. Intracellular recording. J. Neurophysiol. *32*, 339–355.

Zemelman, B.V., Lee, G.A., Ng, M., and Miesenbock, G. (2002). Selective photostimulation of genetically chARGed neurons. Neuron *33*, 15–22.

Zrenner, E. (2002). Will retinal implants restore vision? Science *295*, 1022–1025.